

Cite this: *Energy Environ. Sci.*, 2024, 17, 4508

Developing kilometers-long gravity heat pipe for geothermal energy exploitation†

Wenbo Huang,[‡] Juanwen Chen,[‡] Qingshan Ma,[‡] Linxiao Xing,^e Guiling Wang,^{*e} Jiwen Cen,[‡] Zhibin Li,[‡] Ang Li[‡] and Fangming Jiang[‡]

At medium-deep and deep parts of the Earth's crust lay vast and so far mostly untapped reserves of geothermal energy. This energy source has the potential to meet humanity's needs for energy for thousands of years. However, the large-scale deployment has been hindered by a lack of effective and dependable exploitation technologies. Gravity heat pipes have recently garnered significant attention due to their exceptional heat transfer capability and their ability to harness geothermal heat without water-mining. Nevertheless, it is a persistent challenge to extend gravity heat pipes to depths that are sufficient to exploit deep geothermal energy. In this study, we introduce an innovative ladder-structure inner pipe design to overcome this shortcoming. This design incorporates a series of stepped ladders and small condensate guiding pipes, allowing for the development of super-long gravity heat pipes (SLGHPs). Combined with an optimal working fluid, this novel structure enables kilometers-long gravity heat pipes. As a direct outcome of this innovation, a 4149-meter-long SLGHP was constructed and installed in a geothermal well using ammonia as the working fluid. The SLGHP geothermal system demonstrated the ability of continuous heat output exceeding 1 MW, with a heat flux across the radial section of the SLGHP reaching $4 \times 10^7 \text{ W m}^{-2}$. Furthermore, an ammonia vapor-driven power generator was developed and integrated with the SLGHP system. During a 72-hour test, this generator successfully produced electricity at a steady rate of approximately 7 kW. The breakthrough design of the SLGHPs holds the potential to unlock Earth's deep geothermal energy reserves, providing a sustainable and reliable energy source for generations to come.

Received 18th March 2024,
Accepted 30th April 2024

DOI: 10.1039/d4ee01235f

rsc.li/ees

Broader context

The super-long gravity heat pipe (SLGHP) is a novel and promising technological advancement to exploit medium-deep to deep geothermal energy. We present an innovative design that enables the successful development of a kilometers-long gravity heat pipe to access earth-deep geothermal energy. The SLGHP geothermal system built here is in Xiong'an, China; this heat pipe is the longest in the world with a length of 4149 m. The SLGHP uses ammonia as the working fluid, and the integrated power generator is driven by ammonia vapor generated by the SLGHP. The SLGHP geothermal system can continuously produce more than 1 MW of heat, and the heat flux across the radial cross-section of the heat pipe amounts to $4 \times 10^7 \text{ W m}^{-2}$, surpassing the heat dissipation flux of modern electronic components, which attests to the exceptional heat transfer capability of the developed SLGHP. The world's first SLGHP pilot power generator steadily generated electricity at $\sim 7 \text{ kW}$ rate in a 72 h test. The SLGHP system is expected to be widely deployed for geothermal energy exploitation (power generation and space heating) and for other industrial utilizations, such as underground coal fire control and heavy oil mining.

^a Laboratory of Advanced Energy Systems, Guangzhou Institute of Energy Conversion, Chinese Academy of Sciences (CAS), Guangzhou 510640, China. E-mail: jiangfm@ms.giec.ac.cn

^b CAS Key Laboratory of Renewable Energy, Guangzhou 510640, China

^c Guangdong Provincial Key Laboratory of New and Renewable Energy Research and Development, Guangzhou 510640, China

^d School of Energy Science and Engineering, University of Science and Technology of China, Hefei 230026, China

^e Institute of Hydrogeology and Environmental Geology, Chinese Academy of Geological Sciences, Shijiazhuang 050061, China. E-mail: wangguiling@mail.cgs.gov.cn

^f University of Chinese Academy of Sciences, Beijing 100049, China

† Electronic supplementary information (ESI) available. See DOI: <https://doi.org/10.1039/d4ee01235f>

‡ These authors contributed equally to this work and should be considered as co-first authors.



Introduction

Geothermal energy is a clean and abundant resource that could play a crucial role in addressing global energy shortages, air pollution, and climate change.^{1–4} Hot dry rock (HDR) formations, located 3–10 km beneath the Earth's crust, hold vast reserves of geothermal energy (Fig. S1, ESI[†]), but traditional extraction methods face significant challenges in accessing these reserves. Enhanced geothermal systems (EGSs) were developed in the 1970s to extract heat from HDRs,^{5–7} but they encountered hurdles, such as large-scale rock fracturing^{8,9} and induced micro-seismicity.^{10–14} The growing demand for deep geothermal energy urgently calls for advanced, highly efficient geothermal heat extraction technologies.^{15,16} Moreover, direct geothermal utilization *via* traditional methods commonly involves underground hot water extraction, which faces major challenges, such as geographic limitations,^{17,18} reinjection restrictions,¹⁹ and thermal and chemical pollution due to improper disposal of wastewater.²⁰

Heat pipes are known for their exceptional heat transfer capabilities,^{21–23} and thus, they have been successfully applied in almost all thermal engineering domains, such as solar collectors,^{24,25} electronics cooling,²⁶ energy recovery systems,²² as well as geothermal energy exploitation.^{27,28} They have emerged as a potential solution for deep geothermal energy extraction. The super-long gravity-assisted heat pipe (SLGHP) is an innovative variant of heat pipes to extract geothermal energy from significant depths,²⁹ and it relies on gravity to return the condensed working fluid, eliminating the need for a wick^{30,31} (Fig. S2, ESI[†]). Geothermal systems with the SLGHP are straightforward and do not require pumping mechanisms, making them an attractive alternative to multi-well extraction and reinjection systems, such as the EGS. Moreover, the enclosed and isolated working fluid within the heat pipe minimizes technical challenges associated with traditional methods. In its operation, the working fluid absorbs heat in the evaporation section, vaporizes and rises towards the condensation section, where it condenses and releases heat. The condensate returns to the evaporation section under the action of gravity, sustaining a continuous cycle. As the working fluid primarily absorbs heat in the form of latent heat, the fluid temperature within the heat pipe remains almost unchanged. This feature allows for maximized temperature differences between the heat pipe and surrounding geothermal formation, leading to optimized heat harvesting. Moreover, the SLGHP system minimizes the potential risks of scale/corrosion and loss of the working fluid, resulting in reduced maintenance demands and a diminished environmental footprint. SLGHP systems offer the unique advantage of direct steam production, which can be harnessed for heat pump space heating or steam turbine power generation, eliminating the requirement of supplementary equipment, such as a steam separator or flash evaporator.^{32–34} This enhances the SLGHP efficiency and system performance as compared to conventional geothermal systems.³³

Despite its wide-spectrum applications, heat pipe technology has almost been stagnant in the last two decades.³⁵ In particular, there have been no innovative breakthroughs in

the development of sufficiently long gravity heat pipes that could meet requirements for earth-deep geothermal (*e.g.* HDR) heat extraction; the length of heat pipes rarely surpasses the 100-meter level.³⁶ Gravity heat pipes exceeding this length have been primarily confined to experimental stages and have not demonstrated the consistent performance required for widespread industrial and field use.^{32,37,38} The effectiveness of heat pipes depends on efficient evaporation and condensation in the evaporator and condenser, as well as minimal resistance to vapor flow. The extra-long configuration of the SLGHP, probably spanning a few kilometers, introduces critical limitations.³⁹ Issues, such as undesirable in-pipe flow patterns and substantial pressure drop, arise.⁴⁰ Long-distance vapor/liquid countercurrent flow can cause interphase entrainment and enhanced vapor drag, resulting in ill performance and even failure of the system. The accumulation of liquid, extending to a deep liquid pool, creates obstacles, such as high static hydraulic pressure that inhibits evaporation, leading to startup failures or reduced performance.⁴⁰ Moreover, the pressure drop in the flow of the rising vapor due to frictional and gravitational resistances is negligible in typical “short” heat pipes, but it is notably large and exerts a detrimental impact on the operation of the SLGHPs with lengths of several kilometers.⁴¹ Addressing these challenges necessitates the development of a tailored configuration, which distinctly departs from conventional heat pipe designs, to control in-pipe flow patterns, along with a systematic selection of the working fluid.⁴²

Herein, we present an innovative structural design, which enables the effective performance of kilometers-long SLGHPs. This novel design (Fig. 1) incorporates a set of in-pipe functional modules that couple the stepped reflux configuration with liquid–vapor separation design to achieve highly efficient evaporation and prevent the entrainment of long-distance liquid/vapor counter-flow. A 4149-m-long heat pipe was developed in-house; this is the longest ever reported pipe, which was installed in a geothermal well in Xiong'an New Area, Hebei Province, China. The SLGHP was charged with ammonia as the working fluid; an ammonia vapor-driven power generator was developed and assembled with the SLGHP system. In operation, the SLGHP geothermal system can continuously produce more than 1 MW of heat, and the heat flux through the radial cross-section of the heat pipe amounts to $4 \times 10^7 \text{ W m}^{-2}$, surpassing the typical heat dissipation fluxes of modern electronic components.⁴³ The world's first SLGHP pilot power plant steadily generated electricity at $\sim 7 \text{ kW}$ rate in a 72-hour test. As global energy demands continue to rise, the development of advanced technologies, such as the SLGHPs, will be essential in harnessing the full potential of geothermal energy. By providing a sustainable and efficient means of geothermal energy extraction, the SLGHPs can play a pivotal role in meeting the world's energy needs while mitigating environmental impacts.

SLGHP development

To tap into deep geothermal energy reserves, we have developed an SLGHP capable of reaching lengths of up to a few kilometers.





Fig. 1 Super-long gravity heat pipe and its working principle.

The unique configuration and working principle of the SLGHPs are illustrated in Fig. 1. Featuring a pipe-in-pipe design, the SLGHP incorporates a stepped ladder structure within the inner pipe. Each unit module of the stepped ladder consists of a single inner pipe step and small condensate guiding pipe. One step of the inner pipe and outer casing pipe form an annular container, which can hold the working fluid in the SLGHP. The small guiding pipe regulates the depth of liquid accumulation within the annular container as it facilitates the reflux of the working fluid. Each ladder module measures approximately 10 meters in height, with an assembled small guiding pipe length of 3–4 meters. Multiple ladder modules are strategically arranged within the SLGHP evaporation section. Along the longitudinal direction of the SLGHP, a small gap is intentionally left between neighboring modules to guide vapor flow into the central passage. This innovative stepped ladder structure enables the SLGHP to harness deep geothermal energy efficiently and maintain a continuous cycle of heat absorption, vaporization, condensation, and reflux.

Once filled with an appropriate amount of working fluid, the liquid primarily resides within stepped annular containers, with minimal accumulation at the bottom of the SLGHP. During operation, the working fluid evaporates and enters the central passage, where the vapor flows upwards, and the liquid condensate is directed downwards within the annular space. Liquid accumulation is maintained at an optimal level in the annular containers to ensure complete wetting of the SLGHP evaporation section. Liquid accumulation in the annular containers is not very high, but it is sufficient to keep all SLGHP evaporation sections fully wetted. This novel structure effectively helps address common issues encountered in extra-long gravity heat pipes, such as vapor/liquid entrainment and boiling suppression caused by stagnant liquid pools. The innovative design facilitates highly efficient evaporation and boiling of the working fluid while segregating the flow of liquid and vapor

components; this mitigates the long-range vapor/liquid countercurrent interference. One remaining challenge that may affect SLGHP performance is the resistance imposed on the vapor flow. Long-distance vapor flow can suffer from substantial resistance due to gravity and viscous forces. To counteract the effects of large vapor flow resistance, it is essential to select an optimal working fluid for the SLGHP.

Previous research⁴⁰ proposed that a temperature gradient of the working fluid should be applied along the SLGHP axis (dT/dy) and should be used as a selection criterion. Smaller dT/dy values indicate a better working fluid. It was found that dT/dy remains relatively insensitive to changes in heat pipe diameter and geothermal source temperature, when ammonia is used as the working fluid. However, dT/dy increases significantly for small pipe diameters and low source temperatures with water. Further studies⁴⁴ have revealed the unique phenomenological mechanisms of the SLGHPs by comparing them with normalized gravity heat pipes (NSGHPs). Operational characteristics were analysed in these studies by taking into consideration their distinctive geometric features. While thermal resistance caused by vapor flow is negligible in the NSGHPs, it dominates the overall thermal resistance of the SLGHPs. Both studies^{40,44} concluded that an ideal SLGHP working fluid should possess following properties: (i) high latent heat of vaporization and (ii) a strong dependence of saturated vapor pressure on temperature. A comprehensive analysis has indicated that ammonia is an optimal working fluid for most geothermal applications (Fig. S3, ESI[†]).

SLGHP geothermal system

We built the SLGHP geothermal system in Xiong'an New Area, Hebei Province, China (extended data Fig. 1). The 4507-m-deep geothermal well, D34, is located at Liulizhuang Town, Anxin



County of Xiong'an New Area; geologically, this well is situated in the northeastern part of the Gaoyang Low Uplift within the Jizhong Depression (Fig. S4, ESI†). Based on regional exploration data, the local constant temperature stratum is approximately 25 m below the surface, where a constant temperature of 15 °C is observed. Owing to lithology and tectonic variations, the geothermal gradient varies significantly with depth. The Cenozoic stratum, 0–3455 meters subsurface, primarily consists of loam, mudstone, sandstone, and conglomerate, and it has an average geothermal gradient of 2.73 °C per 100 meters. In contrast, the Proterozoic stratum, 3455–4507 meters subsurface, is predominantly composed of dolomite and has an average geothermal gradient of 1.23 °C per 100 meters. The measured temperature is 131.8 °C at the bottom of the well.

The D34 well was drilled by the China geological survey; its borehole featured three distinct sections with progressively smaller diameters as it reached downward; each section was reinforced with a casing. The first section is at a depth from 0 to 1012 meters with a casing diameter of 339.7 mm; the second extends from a depth of 1012 to 3433 meters with a casing diameter of 244.5 mm; the third is between the depths of 3433 and 4507 meters with a casing diameter of 177.8 mm. An SLGHP developed in-house with a length of 4149 meters was installed inside the wellbore (Fig. 2b). The SLGHP also consists of three sections with different outside diameters: (1) from 0 to 752 meters in depth, the diameter is 244.5 mm; (2) from 752 to 3105 meters, the diameter is 177.8 mm; and (3) from 3105 to 4149 meters, the diameter is 127.0 mm. Each section of the SLGHP is slightly smaller in diameter than the corresponding borehole casing. To eliminate the thermal contact resistance between the SLGHP and geothermal formations, the annular space between the SLGHP and casing was filled with water. It should be mentioned the SLGHP is about 350 meters shorter than the well depth, which helps protect the SLGHP and wellbore from potential damage.

The pilot SLGHP geothermal system is schematically presented in Fig. 2(a). It was designed to serve two sets of tests: heat extraction test and power generation test. For the heat extraction test, valves 1 and 4 are turned on, while valves 2, 3, 5, and 6 are turned off. This arrangement allows the vapor of the working fluid to leave the SLGHP and flow directly into the condenser, releasing latent heat into cooling water. Subsequently, the condensed fluid, after returning to the SLGHP, flows into it by the force of gravity. The heated cooling water goes to the cooling tower and releases heat to the ambient atmosphere. For the power generation test, valves 2, 3, 5, and 6 are turned on, while valves 1 and 4 are turned off. In this setup, the vapor of the working fluid coming from the top of the SLGHP flows into a double-stage turbine and later into the condenser. The condenser is cooled by circulating water; as a result, the pressure of the working fluid in the condenser is significantly lower than the pressure of the vapor leaving the SLGHP and entering the condenser. This pressure difference causes the working fluid vapor to expand, while going through the turbine, which drives the generator to produce electricity. The condensed fluid in the condenser is collected in a tank, and subsequently, re-introduced into the SLGHP by a booster pump. For both tests, cooling water circulates first through the condenser and is then sent to the cooling tower to lower its temperature to the required level before entering the condenser. The performance of the cooling tower is adjusted by controlling the operation of two air fans positioned at its top. Adjusting the speed of these fans can create various cooling conditions for the tests.

Considering the geothermal conditions and size of the SLGHP, ammonia was selected as the working fluid for the heat pipe⁴² (Fig. S3, ESI†). Before charging with ammonia, the SLGHP was vacuumed to a vacuum level lower than 0.8 kPa. The SLGHP was charged (or discharged) many times with

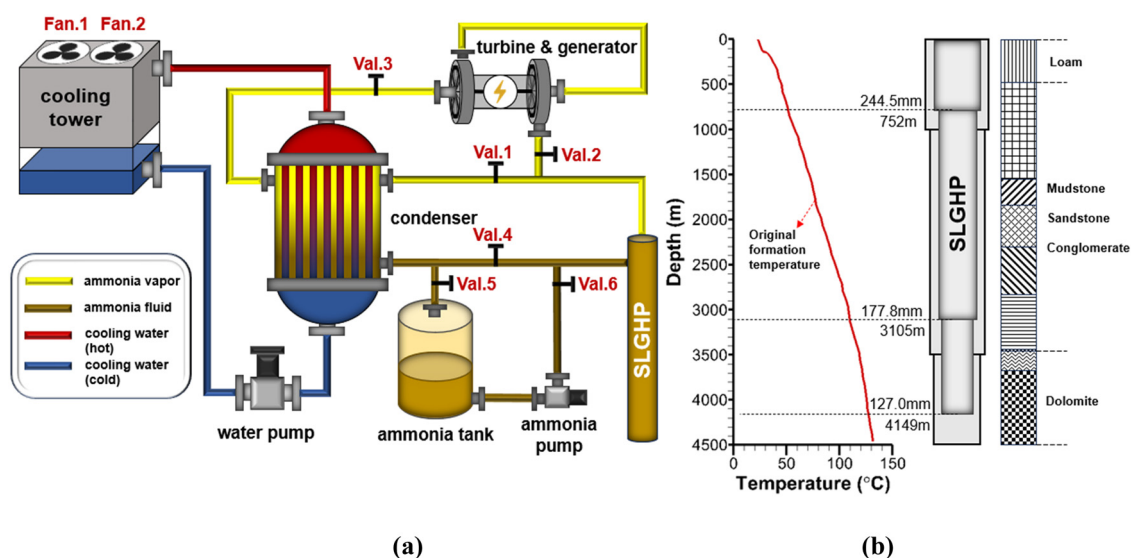


Fig. 2 (a) SLGHP geothermal system constructed in Xiong'an, China; (b) measured temperature in the original geothermal formation, well-borehole configuration after assembly with the SLGHP, and local geological formation.



ammonia; each time, while charging or discharging, about 200–500 kg of ammonia was used, and the pressure in the SLGHP condenser was recorded 24 hours after each charge (or discharge). We checked the pressure in the SLGHP condenser to examine the response of the SLGHP to the charge (or discharge) with ammonia to verify proper operation.

Fig. 3a demonstrates the pressure in the SLGHP condenser as a function of the amount of ammonia in the SLGHP, and Fig. 3b schematically presents the calculated ammonia distribution in the SLGHP at different stages. Regardless of the amount of ammonia used for charge or discharge, qualitatively, the pressure in the condenser increases with increasing amounts of ammonia in the SLGHP, while the ammonia distribution shows three distinct stages: I. Vapor only; II. Partially wetted; and III. Fully wetted.

In the vapor-only stage, all the ammonia in the SLGHP is in the vapor phase. Once charged ammonia, which turns into vapor immediately, is sufficient to fill all the space in the SLGHP, liquid ammonia starts to accumulate at the uppermost ladder module. In Fig. 3a, it can be noted the vapor-only stage ends at a condenser pressure of 1.2 MPa with charging using approximately 0.45 tons of ammonia. 1.2 MPa pressure corresponds to the saturation vapor pressure of ammonia at the geothermal formation's original temperature (31 °C) at the location of the upper first ladder. The increase in ammonia charged into the SLGHP leads to the filling of the upper ladder modules with liquid ammonia, while the pressure in the condenser increases. Inside the SLGHP, the temperature is almost uniform; the operation of the partially-wetted SLGHP flattens the geothermal formation temperature of the wet section. In Fig. 3a, it is worth noting that the partially-wetted stage occurs for an ammonia quantity of 4.68 tons, at which point liquid ammonia reaches the position of approximately 2000 m underground. By further increasing the amount of ammonia charged, the wet section progressively extends deeper. As the average formation temperature across the wet section increases, the temperature in the SLGHP, and the pressure in the condenser also increases. When all ladder

modules in the SLGHP are filled with liquid ammonia, the temperature and pressure in the SLGHP reach the highest values; the highest recorded pressure in the condenser is 3.97 MPa with 7.70 tons of ammonia charged, as illustrated in Fig. 3a. The SLGHP system was charged with ammonia one more time, amounting to a total of 7.93 tons of ammonia. It is observed that the pressure decreases, which occurs because too much liquid ammonia accumulates and floods the SLGHP bottom section, hindering the evaporation of ammonia.⁴⁵ The pressure for the ammonia discharge process (Fig. 3a) is always above that for the charging process, which is due to substantially more heat uptake from the deeper high-temperature geothermal formation during the discharge process. For 0.45 tons of ammonia, no liquid ammonia remains in the SLGHP, and the pressure for the charge and discharge process coincide.

The above-described charge/discharge tests corroborate that the SLGHP can properly work according to its design, and it is found that the SLGHP needs 7.70 tons of ammonia for its optimum filling.

Performance of the SLGHP geothermal system

Performance tests of the SLGHP geothermal system spanned over a period of about 170 days, including a 40-day continuous heat extraction test, a 45-day continuous heat extraction test, a 3-day power generation test, and an 80-day continuous heat extraction test (extended data Fig. 2). In total, the 3-stage heat extraction test lasted for more than 165 days and was conducted for three different speed levels of cooling tower fans, namely: (I) full speed, (II) medium speed, and (III) low speed. 40-Day testing data for each of the three testing conditions is reported in Fig. 4a. Lowering the fan speed increases the temperature at which ammonia vapor condenses and SLGHP production temperature, while it decreases the heat extraction rate. As the heat extraction test proceeds, the heat extraction

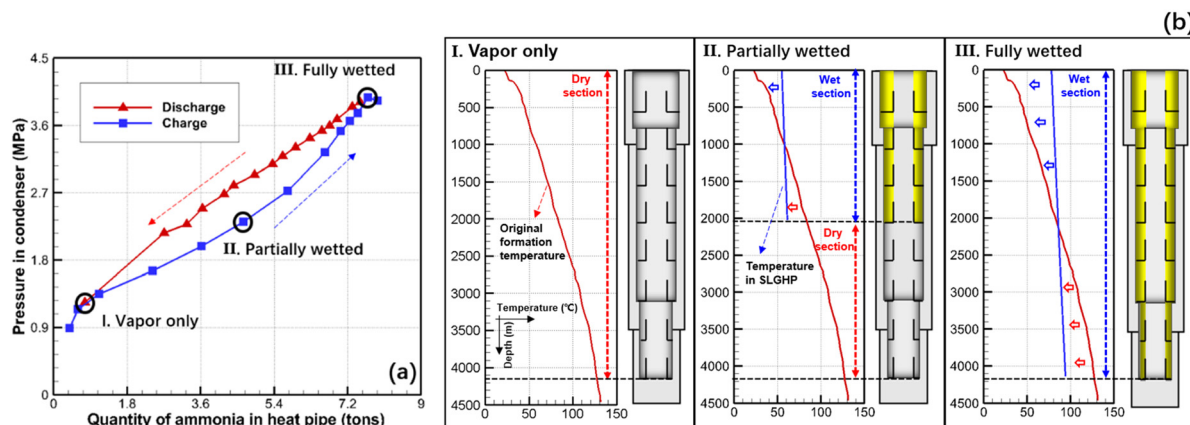


Fig. 3 Response of the SLGHP to charge and discharge with ammonia. (a) Pressure in the SLGHP condenser as a function of the ammonia quantity; (b) schematic distribution of ammonia in the SLGHP.



rate tends to decrease, primarily due to the declining geothermal formation temperature adjacent to the SLGHP. This occurrence is common for single-well closed-loop geothermal systems.⁴⁶

Under test conditions I, II and III, 40-day average production temperatures are 36.8 °C, 52.8 °C, and 59.3 °C, respectively. The corresponding average heat extraction rates over the 40-day test are 1049 kW, 596 kW, and 442 kW, respectively. In terms of the diameter of the middle section of the heat pipe, 177.8 mm, considering the 1049 kW heat extraction rate, the heat flux through a radial cross-section of the SLGHP is more than $4 \times 10^7 \text{ W m}^{-2}$, attesting its exceptional heat transfer capability. The simulated heat extraction rates (at each production temperature, 40-day averaged), along with the data of the three tests are reported in Fig. 4b. The simulation model employed (Fig. S5, ESI[†]) is detailed in the ESI[†] which has already been validated by practical field test data⁴⁷ and was further validated by underground temperatures measured in the present work (extended data Fig. 3). Close observation of Fig. 4b has evidence that simulation results, and test data agree well with each other. The simulation model is based on the assumption that the SLGHP operates under ideal conditions, in particular, by assuming that liquid/vapor entrainment, stagnant liquid at the SLGHP bottom, and local dry-outs do not occur. Therefore, the good agreement between the test data and simulation results

indicates the SLGHP design is very successful as it leads to a system performing close to an ideal system.

In addition to condenser temperatures, Fig. 4c reports SLGHP temperatures measured at three underground monitoring points, *i.e.*, at 235 m, 470 m, and 940 m subsurface, respectively, under the conditions of test II. As the heat extraction process proceeds, the temperature of the SLGHP decreases as a result of the decrease in the temperature of the surrounding geothermal formation. The temperature of the upward flow in the SLGHP, from underground to surface, decreases but, generally, the decrease is relatively minor – about 5 °C for a distance of approximately 1000 m. Inside the SLGHP, the ammonia vapor and liquid are thermodynamically in a quasi-equilibrium state; therefore, the temperature and pressure are related to each other (Fig. S6, ESI[†]), *i.e.* the temperature decrease is essentially associated with the drop in vapor pressure. The measured drop in temperature indicates that the SLGHP is performing very well; furthermore, observations in Fig. 4a lead to the conclusion that control of the temperature in the condenser is an effective measure to adjust the heat extraction rate of the SLGHP. Extended data Fig. 4 reports the results under the test conditions of I and III.

After the heat extraction tests of the SLGHP system were completed, the geothermal formation was allowed to recover

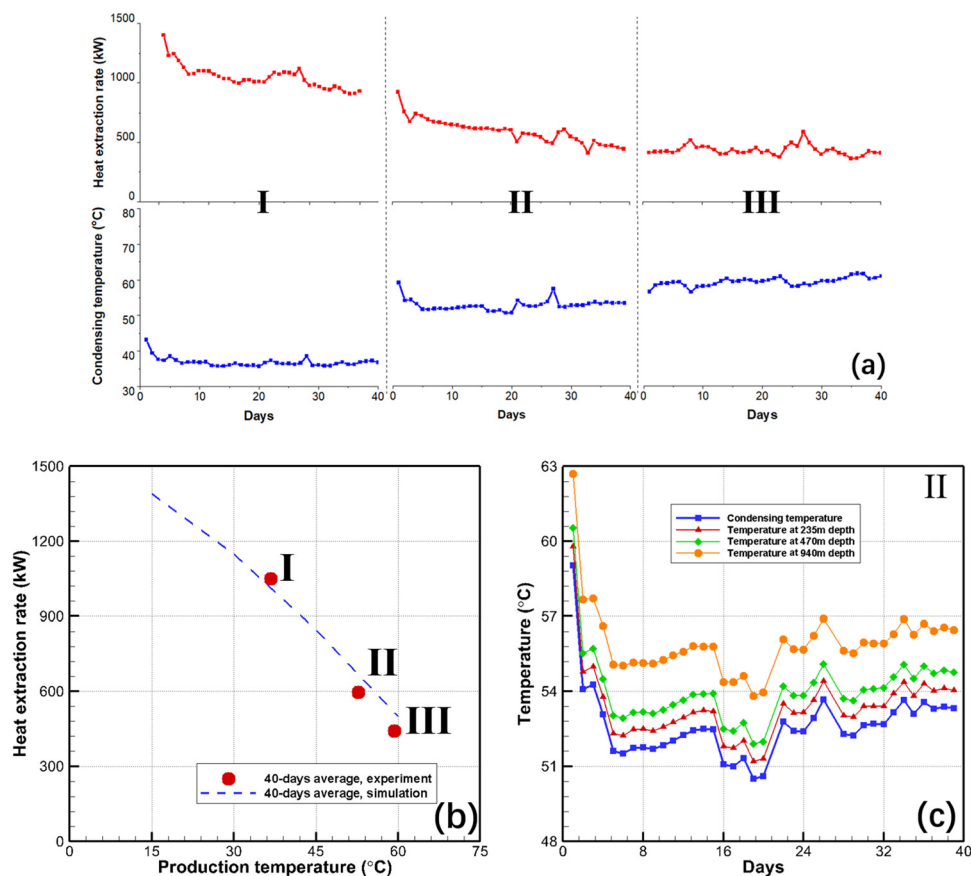


Fig. 4 Heat extraction performance of the SGHLP system. (a) Heat extraction rate and production temperature during 40-day heat extraction tests; (b) comparison of 40-day average heat extraction rates between experimental data and simulation results; (c) SLGHP temperatures measured at three monitoring points underground, *i.e.*, at 235 m, 470 m, and 940 m subsurface, respectively, under the conditions of test II.



for 16 days. During this time, the power generation test was conducted for 72 hours in total. The primary aim of the test is to verify the feasibility of saturated vapor produced by the SLGHP system to drive the steam turbine of the power generation system, which operates as a Rankine cycle. The operation is started by keeping the cooling tower and water circulation loop in an idle state; valves 2, 3, 4, 5, and 6 are then turned on, while valve 1 is turned off. Therefore, pressures before and after the turbine are equal, both in equilibrium with the SLGHP output vapor. By turning off valve 4 and turning on the water pump to start the cooling tower and water circulation loop, the pressure in the condenser decreases, leading to the development of a pressure difference between the two ends of the turbine, which drives the turbine and coaxial electrical generator to produce electricity.

The performance of the SLGHP power generation system is reported in Fig. 5 of extended data; this shows the heat extraction rate, power generation rate, turbine inlet temperature, turbine outlet temperature and ambient temperature as a function of the operation time. In addition, it includes an exergy flow chart, which was calculated in terms of the average values obtained from the 72-hour experiment. A two-stage turbine designed in-house (Fig. 5e) was used for the test. The first and second stages of the turbine share a common shaft with an electrical generator, while they are set with a reverse exhaust direction to counterbalance the axial force. The designed turbine inlet temperature and outlet temperature are 50.6 °C and 37 °C,

respectively. During the 72-hour test, the turbine inlet temperature was kept below the designed value, and the average value was only 46.53 °C (Fig. 5c). Nevertheless, it can be noted the power generation system steadily generates electricity at ~7 kW rate during the test (Fig. 5b). The power generation trend indicates two relevant characteristics: the first is that the power generation increases with an increase in heat extraction rate, although the increase is not obvious due to reduced turbine efficiency (extended data Fig. 6b); the second is that power generation slowly decreases with the operation time, which is similar to the temporal behavior of the heat extraction rate.

The exergy flow chart in Fig. 5d indicates that the total exergy production from the underground geothermal formation was 108.48 kW in the 72-hour test (extended data Fig. 6a). This demonstrates the good potential of the SLGHP power generation system. The largest exergy destruction occurs during the condensation process, which accounts for 73.70% of the total exergy produced. This large exergy destruction is mainly caused by the cooling capacity of the cooling tower, which cannot further reduce the temperature difference between condensation and ambient temperatures. However, this large portion of energy loss can be recovered through cascade utilization systems with different types of output, such as space heating. Moreover, as the ammonia-driven turbine is operating at off-design conditions, its low efficiency (extended data Fig. 6b) is also an important reason causing the low exergy efficiency of the SLGHP power generation system (extended data Fig. 6c).

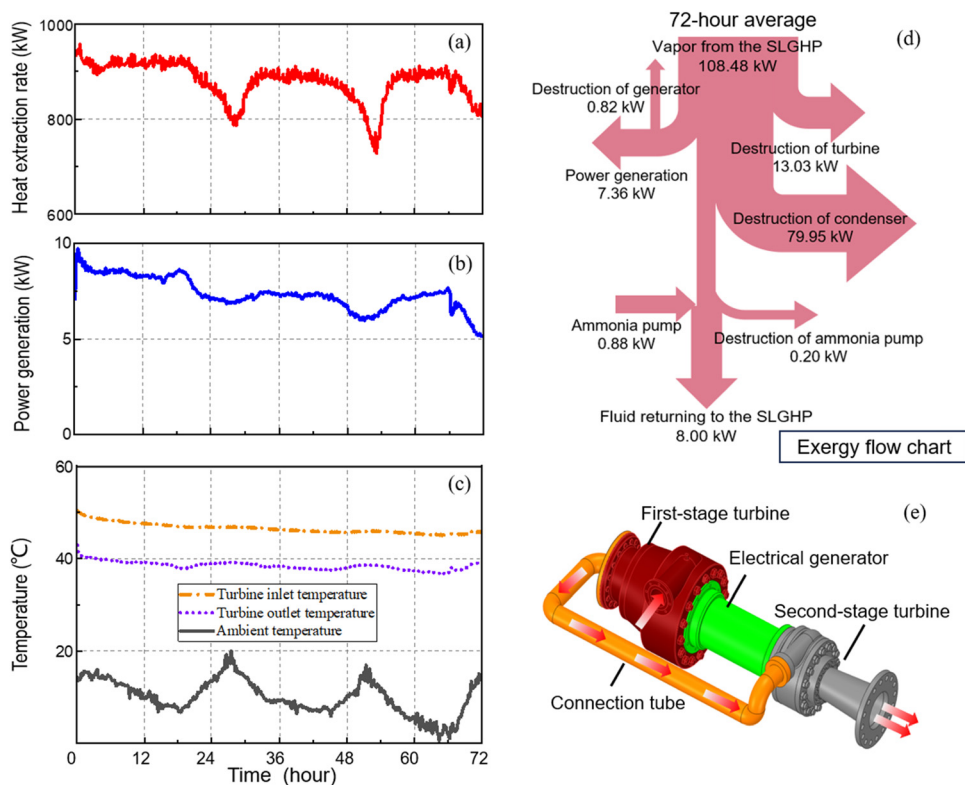


Fig. 5 Power generation performance of the SLGHP system. (a) Heat extraction rate, (b) power generation, (c) temperatures, (d) exergy flow chart, and (e) turbine structure.



Concluding remarks

Conventional technologies for the extraction of geothermal energy have faced serious drawbacks in their development and utilization. In particular, the mining-water-to-use-heat mode for hydrothermal resource exploitation has caused numerous secondary environmental problems, such as decreased underground water levels, surface subsidence and adverse environmental impact.²⁰ The Enhanced Geothermal System (EGS) for HDR heat extraction has made slow progress toward commercialization due to several difficulties, such as artificial reservoir creation, downhole interwell-connection^{8,9} and induced seismic activity.^{10–14} Using the SLGHP to exploit medium-deep and deep geothermal resources circumvents or even avoids issues or technical difficulties encountered in accessing conventional hydrothermal energy and EGS exploitation from the HDR. The kilometers-long SLGHP developed in the present work is expected to be widely deployed for geothermal energy exploitation.

Using SLGHP facilitates heat transport from deep into the earth to the ground; the tests conducted to evaluate the SLGHP geothermal system have demonstrated the exceptional heat transfer capability of the SLGHP. However, the low thermal conductivity of the geothermal formation can limit the overall heat extraction performance of SLGHP geothermal systems.⁴⁸ The augmentation of the SLGHP heat production is a challenge, which must be addressed. The creation of near-well artificial reservoirs, in combination with heat transfer enhancement, can offer a potential solution. Previous studies^{29,48} indicate that near-well heat transfer enhancement within a ~10-meter radius around the SLGHP can effectively augment its performance.

The SLGHP geothermal systems have the unique advantage of direct vapor production, which can be used to drive heat pump systems for space heating or steam turbines for power generation, simplifying the surface-level systems for geothermal utilization. At the same time, it enhances the energy utilization efficiency. Testing of the SLGHP ammonia vapor-driven power generation system demonstrates the feasibility of this technological route; however, it should be accepted that there is still much research work to be done in the future, such as optimization and adaptation of the design of the surface equipment and steam turbine.

For large-scale commercial deployment, we may first consider the geothermal energy exploitation from numerous abandoned oil/gas wells to save the well-drilling cost, which can be the largest initial investment in the SLGHP geothermal systems.^{49,50} The SLGHP is essentially a highly efficient heat transport device, which can be also used in industrial scenarios, other than geothermal energy production, for instance, underground coal fire control⁵¹ and heavy oil mining.^{52,53}

Methods

SLGHP fabrication

The SLGHP was fabricated by assembling many standard oil casing tubes of ~11 m in length; the casing tubes are connected by screw joints. The total length of the gravity heat pipe

is 4149 m, consisting of 3 sections of 244.5 mm (0–752 m), 177.8 mm (752–3105 m) and 127.0 mm (3105–4149 m) outer diameter, respectively. Fig. 1 presents details of the stepped ladder module, which was welded inside each casing tube.

Installment of the SLGHP geothermal system

Standard oil casing tubes (~11 meters in length) welded with inner pipes are manufactured as modular products. These are placed inside the well one-by-one after being connected by screw joints. On the ground, the SLGHP is connected to the condenser; power generator and cooling tower to complete the SLGHP geothermal system (Fig. 2).

Temperature measurements

The downhole temperatures of the SLGHP are measured by a multi-point temperature detection system composed of several probes and a cable connected to a host. The instrument model is SYKJ-16, produced by Shanxi Gentry Yu Electronic Technology Co. Ltd. The error in temperature measurements is ± 0.5 °C. Three temperature probes were mounted on the outer surface of the heat pipe. The depths of these probes are 235 m, 470 m and 940 m, respectively. Temperatures of ground devices are measured by plug-in Pt resistance temperature probes attached to specified monitoring positions, which have a measuring error of ± 0.1 °C.

Pressure measurement

A pressure sensor was set in the condenser to collect and send pressure data to a data acquisition system. The pressure transmitter is a product of Shanghai Enbbon Automation Instrument Co. Ltd, model type EB3351T-G, with a measuring range of 0–6 MPa and an uncertainty of $\pm 0.2\%$ FS (full scale).

Fluid flow rate measurement

The cooling water flow rate is measured by an electromagnetic flowmeter set at the outlet of the condenser. The flowmeter model is LWGY-65C, which is a product of Fimeet Company with a measuring error of $\pm 0.5\%$.

Ammonia charge and discharge

The system is vacuumed before charging with ammonia. During charging, valve 6 is open and valves 4 and 5 are closed (Fig. 2). To guarantee the complete release of gases from the SLGHP, a small amount of ammonia is first injected into the SLGHP by a high-pressure injection pump, followed by discharge and vacuum. This process is repeated a few times to allow a reduced vacuum of <0.8 kPa in the SLGHP, which allows the charging process to proceed. The quantity of ammonia used for charging is monitored by the liquid level gauge set at the ammonia storage tank. The system also allows ammonia vapor to return to the tank (*i.e.* ammonia discharge) when valves 1 and 5 are open and other valves are closed, while the cooling of the condenser is in action by circulating water.



Heat extraction testing

In the heat extraction testing, the SLGHP geothermal system (Fig. 2) has valves 1 and 4 on, while valves 2, 3, 5, and 6 are off. By adjusting the speed of the two cooling tower fans, the temperature at which ammonia condenses and its corresponding saturation pressure inside the condenser is controlled. Different condensing temperatures result in different heat extraction rates. The calculation of the SLGHP system heat extraction rate is determined using eqn (S1) (ESI†).

Power generation testing

In the power generation test, the electricity generated is consumed by an electric heater to heat water. The voltage, current, and frequency are measured and recorded by a digital power meter, model PM9816, produced by NAPU Company, with a measuring error of $\pm 0.5\%$. The real-time power generation is calculated by multiplying voltage and current; the exergy production rate and exergy efficiency, as well as turbine efficiency, are calculated with thermodynamic models reported in ESI,† eqn (S2)–(S7).

SLGHP heat extraction modeling

A previous model^{42,47} was employed to simulate the SLGHP heat extraction process. The framework and governing equations of this model are presented in Fig. S5 (ESI†). The model is formulated based on following assumptions: (i) no stagnant liquid pool or dry spot is present at the bottom of the heat pipe, *i.e.*, no evaporation inhibition or local overheating occurs at the bottom evaporation part of the heat pipe; (ii) no liquid–vapor entrainment occurs along the heat pipe, and thus, the flow resistance in the SLGHP is mainly determined by the flow resistance of the vapor and follows an empirical in-pipe turbulent flow resistance correlation; (iii) the fluid inside the heat pipe is thermodynamically in a phase equilibrium state; (iv) the working fluid condenses at constant temperature (T_c) when leaving the 2nd stage of the turbine and entering the condenser; and (v) the interphase momentum exchange of the gas–liquid phase is neglected. The data from a field test⁴⁷ conducted in Tangshan, Hebei Province, China, was used to benchmark the model and validate its accuracy. In the present study, the SLGHP employs ammonia as the working fluid, while water was used as the working fluid in the SLGHP used in the Tangshan Field test. Therefore, the model was extensively tested using ammonia. The simulation results were compared with the measured temperatures of the three downhole temperature monitoring points (at depths of 235 m, 470 m, and 940 m, respectively) during a 12-hour heat extraction test and 60-hour heat recovery test. The good agreement (extended data Fig. 3) between the simulation results and measurements further corroborates the reliability of the model.

Author contributions

W. B. H., J. W. C., Q. S. M., G. L. W., and F. M. J. wrote the manuscript. W. B. H., J. W. C., and F. M. J. designed and

developed the SLGHP and SLGHP geothermal system. W. B. H., J. W. C., and J. W. C. constructed the SLGHP system in Xiong'an. W. B. H., L. X. X., Z. B. L., and A. L. did the heat extraction test. W. B. H., Q. S. M., Z. B. L., and A. L. did the power generation test. L. X. X. and G. L. W. prepared the geological data. All authors contributed to the organization and preparation of the manuscript, and they participated in ongoing discussions and progress meetings over the duration of the project. All authors have approved the final version of the manuscript, and they consent to its publication.

Data availability

All data generated or analyzed during this study are included in this article, extended data and ESI.†

Conflicts of interest

The authors declare that they are not aware of any known competing financial interests or personal relationships, which could have influenced the work reported in this paper.

Acknowledgements

Financial support received from the National Key R&D Program of China [Grant No. 2021YFB1507301 and 2021YFB1507300] is gratefully acknowledged. The Zhejiang Boxu New Energy Technology Co. Ltd. is acknowledged for its help with the manufacturing and assembling of the ammonia vapor-driven power generation system.

References

- 1 J. W. Tester, K. F. Beckers, A. J. Hawkins and M. Z. Lukowski, The evolving role of geothermal energy for decarbonizing the United States, *Energy Environ. Sci.*, 2021, **14**, 6211–6241.
- 2 M. Alsaleh, Z. Yang, T. Chen, X. Wang, A. S. Abdul-Rahim and H. Mahmood, Moving toward environmental sustainability: assessing the influence of geothermal power on carbon dioxide emissions, *Renewable Energy*, 2023, **202**, 880–893.
- 3 A. E. MacDonald, C. T. Clack, A. Alexander, A. Dunbar, J. Wilczak and Y. Xie, Future cost-competitive electricity systems and their impact on US CO₂ emissions, *Nat. Clim. Change*, 2016, **6**, 526–531.
- 4 P. L. Younger, Missing a trick in geothermal exploration, *Nat. Geosci.*, 2014, **7**, 479–480.
- 5 R. Oxburgh, Energy from warm rocks, *Nature*, 1976, **262**, 526–528.
- 6 L. Odling-Smee, Hot rocks could help meet US energy needs, *Nature*, 2007, DOI: [10.1038/news070122-4](https://doi.org/10.1038/news070122-4).
- 7 D. Davies, USA: rock energy, *Nature*, 1977, **269**, 553.



- 8 M. L. McLean and D. N. Espinoza, Thermal destressing: implications for short-circuiting in enhanced geothermal systems, *Renewable Energy*, 2023, **202**, 736–755.
- 9 P. Olasolo, M. C. Juarez, M. P. Morales, S. D'Amico and I. A. Liarte, Enhanced geothermal systems (EGS): a review, *Renewable Sustainable Energy Rev.*, 2016, **56**, 133–144.
- 10 F. Parisio, V. Vilarrasa, W. Wang, O. Kolditz and T. Nagel, The risks of long-term re-injection in supercritical geothermal systems, *Nat. Commun.*, 2019, **10**, 4391.
- 11 K.-H. Kim, J.-H. Ree, Y. Kim, S. Kim, S. Y. Kang and W. Seo, Assessing whether the 2017 Mw 5.4 Pohang earthquake in South Korea was an induced event, *Science*, 2018, **360**, 1007–1009.
- 12 F. Grigoli, S. Cesca, A. P. Rinaldi, A. Manconi, J. A. Lopez-Comino and J. Clinton, *et al.*, The November 2017 Mw 5.5 Pohang earthquake: a possible case of induced seismicity in South Korea, *Science*, 2018, **360**, 1003–1006.
- 13 S. Westlake, C. H. John and E. Cox, Perception spillover from fracking onto public perceptions of novel energy technologies, *Nat. Energy*, 2023, **8**, 149–158.
- 14 D. Giardini, Geothermal quake risks must be faced, *Nature*, 2009, **462**, 848–849.
- 15 E. Hirvijoki and J. Hirvonen, The potential of intermediate-to-deep geothermal boreholes for seasonal storage of district heat, *Renewable Energy*, 2022, **198**, 825–832.
- 16 R. V. Rohit, R. V. Raj, D. C. Kiplangat, R. Veena, R. Jose and A. P. Pradeepkumar, *et al.*, Tracing the evolution and charting the future of geothermal energy research and development, *Renewable Sustainable Energy Rev.*, 2023, **184**, 113531.
- 17 O. G. Correspondent, Geothermal Power: Harnessing Hot Springs Around the World, *Nature*, 1971, **230**, 209.
- 18 Q. Schiermeier, J. Tollefson, T. Scully, A. Witze and O. Morton, Electricity without carbon, *Nature*, 2008, **454**, 816–824.
- 19 P. Seibt and T. Kellner, Practical experience in the reinjection of cooled thermal waters back into sandstone reservoirs, *Geothermics*, 2003, **32**, 733–741.
- 20 R. C. Axtmann, Environmental Impact of a Geothermal Power Plant: Chemical and thermal effluents from a New Zealand plant rival those from fossil or nuclear fuel technologies, *Science*, 1975, **187**, 795–803.
- 21 C. W. Chan, E. Siqueiros, J. Ling-Chin, M. Royapoor and A. P. Roskilly, Heat utilisation technologies: a critical review of heat pipes, *Renewable Sustainable Energy Rev.*, 2015, **50**, 615–627.
- 22 H. N. Chaudhry, B. R. Hughes and S. A. Gharri, A review of heat pipe systems for heat recovery and renewable energy applications, *Renewable Sustainable Energy Rev.*, 2012, **16**, 2249–2259.
- 23 L. L. Vasiliev, Heat pipes in modern heat exchangers, *Appl. Therm. Eng.*, 2005, **25**, 1–19.
- 24 A. Shafieian, M. Khiadani and A. Nosrati, Strategies to improve the thermal performance of heat pipe solar collectors in solar systems: a review, *Energy Convers. Manage.*, 2019, **183**, 307–331.
- 25 A. Shafieian, M. Khiadani and A. Nosrati, A review of latest developments, progress, and applications of heat pipe solar collectors, *Renewable Sustainable Energy Rev.*, 2018, **95**, 273–304.
- 26 Y.-W. Chang, C.-H. Cheng, J.-C. Wang and S.-L. Chen, Heat pipe for cooling of electronic equipment, *Energy Convers. Manage.*, 2008, **49**, 3398–3404.
- 27 G. Deng, N. Kang, J. He, S. Wang, G. Liu and N. Liu, An investigation of the performance of groundwater-based heat pipes in heating lawn systems, *Energy Convers. Manage.*, 2021, **244**, 114492.
- 28 X. Wang, Y. Wang, Z. Wang, Y. Liu, Y. Zhu and H. Chen, Simulation-based analysis of a ground source heat pump system using super-long flexible heat pipes coupled bore-hole heat exchanger during heating season, *Energy Convers. Manage.*, 2018, **164**, 132–143.
- 29 W. Huang, W. Cao and F. Jiang, A novel single-well geothermal system for hot dry rock geothermal energy exploitation, *Energy*, 2018, **162**, 630–644.
- 30 B. Zohuri, *Heat pipe design and technology*. Springer, Cham, 2016.
- 31 D. Reay, P. Kew and R. McGlen, *Heat pipes: theory, design and applications*, Elsevier Ltd, 6th edn, 2014.
- 32 A. Franco and M. Vaccaro, On the use of heat pipe principle for the exploitation of medium-low temperature geothermal resources, *Appl. Therm. Eng.*, 2013, **59**, 189–199.
- 33 Q. Ma, W. Huang, J. Chen, J. Cen, Z. Li and W. Lin, *et al.*, Thermodynamic and economic performance of super-long gravity heat pipe geothermal power plant, *Appl. Therm. Eng.*, 2024, **248**(6), 123115.
- 34 Q. Ma, J. Chen, W. Huang, Z. Li, A. Li and F. Jiang, Power generation analysis of super-long gravity heat pipe geothermal systems, *Appl. Therm. Eng.*, 2024, **242**, 122533.
- 35 W. Chang, G. Huang, K. Luo, P. Wang and C. Li, Ultra-efficient heat pipes enabled by nickel-graphene nanocomposite coatings: concept and fundamentals, *Carbon*, 2022, **191**, 384–392.
- 36 T. Lin, X. Quan and P. Cheng, Experimental investigation of superlong two-phase closed thermosyphons for geothermal utilization, *Int. J. Therm. Sci.*, 2022, **171**, 107199.
- 37 J. C. Ebeling, X. Luo, S. Kabelac, S. Luckmann and H. Kruse, Dynamic simulation and experimental validation of a two-phase closed thermosyphon for geothermal application, *Propulsion Power Res.*, 2017, **6**, 107–116.
- 38 J.-C. Ebeling, S. Kabelac, S. Luckmann and H. Kruse, Simulation and experimental validation of a 400 m vertical CO₂ heat pipe for geothermal application, *Heat Mass Transfer*, 2017, **53**, 3257–3265.
- 39 J. Seo, I. C. Bang and J. Y. Lee, Length effect on entrainment limit of large-L/D vertical heat pipe, *Int. J. Heat Mass Transfer*, 2016, **97**, 751–759.
- 40 J. Chen, J. Cen, W. Huang and F. Jiang, Multiphase flow and heat transfer characteristics of an extra-long gravity-assisted heat pipe: an experimental study, *Int. J. Heat Mass Transfer*, 2021, **164**, 120564.
- 41 T. Gao, X. Long, H. Xie, L. Sun, J. Wang and C. Li, *et al.*, A discussion of internal flow characteristics and performance of super long gravity heat pipes for deep geothermal energy extraction, *Appl. Therm. Eng.*, 2024, **236**, 121557.



- 42 J. Chen, W. Huang, J. Cen, W. Cao, Z. Li and F. Li, *et al.*, Heat Extraction from Hot Dry Rock by Super-long Gravity Heat Pipe: Selection of working fluid, *Energy*, 2022, **255**, 124531.
- 43 R. Van Erp, R. Soleimanzadeh, L. Nela, G. Kampitsis and E. Matioli, Co-designing electronics with microfluidics for more sustainable cooling, *Nature*, 2020, **585**, 211–216.
- 44 J. Chen, W. Huang, J. Cen, Z. Li, F. Li and A. Li, *et al.*, Operational Characteristics of the Super-long Gravity Heat Pipe for Geothermal Energy Exploitation, *Appl. Therm. Eng.*, 2023, **236**, 121530.
- 45 D. Jafari, A. Franco, S. Filippeschi and P. Di Marco, Two-phase closed thermosyphons: a review of studies and solar applications, *Renewable Sustainable Energy Rev.*, 2016, **53**, 575–593.
- 46 Y. Luo, G. Xu and N. Cheng, Proposing stratified segmented finite line source (SS-FLS) method for dynamic simulation of medium-deep coaxial borehole heat exchanger in multiple ground layers, *Renewable Energy*, 2021, **179**, 604–624.
- 47 W. Huang, J. Cen, J. Chen, W. Cao, Z. Li and F. Li, *et al.*, Heat Extraction from Hot Dry Rock by Super-long Gravity Heat Pipe: A Field Test, *Energy*, 2022, **247**, 123492.
- 48 Z. Li, W. Huang, J. Chen, J. Cen, W. Cao and F. Li, *et al.*, An enhanced super-long gravity heat pipe geothermal system: conceptual design and numerical study, *Energy*, 2023, **267**, 126524.
- 49 L. Santos, A. D. Taleghani and D. Elsworth, Repurposing abandoned wells for geothermal energy: current status and future prospects, *Renewable Energy*, 2022, **194**, 1288–1302.
- 50 Y. L. Nian and W. L. Cheng, Insights into geothermal utilization of abandoned oil and gas wells, *Renewable Sustainable Energy Rev.*, 2018, **87**, 44–60.
- 51 X. Zhou, L. Guo, Y. Zhang, Z. Wang, Y. Ma and X. Li, Feasibility investigation of utilizing spontaneous combustion energy of abandoned coal gangue by constructing a novel artificial heat reservoir, *J. Cleaner Prod.*, 2022, **373**, 133948.
- 52 C. Ma, X. Wu and S. Gao, Analysis and applications of a two-phase closed thermosyphon for improving the fluid temperature distribution in wellbores, *Appl. Therm. Eng.*, 2013, **55**, 1–6.
- 53 X. Zhang and H. Che, Reducing heat loss of fluids in heavy oil wellbore using two-phase closed thermosyphon sucker rod, *Energy*, 2013, **57**, 352–358.

